Available online at www.sciencedirect.com

ScienceDirect

Transportation Research Procedia 70 (2023) 154–161

Transportation Research Procedia

www.elsevier.com/locate/procedia

8th International Electric Vehicle Conference (EVC 2023)

Power Electronics Converters for an Electric Charging Station: Description and Experimental Evaluation

Moacyr A. G. de Brito, Anderson S. Volpato, Edson A. Batista and Ruben B. Godoy*

Electrical Engineering Department, Faculty of Engineering, Architecture and Urbanism and Geography – FAENG, Federal University of Mato Grosso do Sul – UFMS, Campo Grande-MS, Brazil

Abstract

This paper presents the power electronics converters of an electric vehicle charging station that works as a DC microgrid with an AC grid interface. The interface converter is an interleaved bidirectional DC-AC converter that enables the V2G (vehicle-to-grid) application. Inside the microgrid, there are converters for managing power from the DC bus to the electrical vehicles (wireless charging type) and stationary battery banks – all bidirectional, too. To constitute the sustainable characteristic of the solution, a solar photovoltaic system is attached to the DC bus through a power electronics converter. The control methodology and experimental results from the proposed system with focus on the converters characteristics are presented. This manuscript highlights a noteworthy reduction in the total harmonic distortion for the injected grid current as well as enhanced stability during battery charging and discharging in both wired and wireless modes.

Keywords: Electric vehicle charging station, microgrid, power electronics converters, V2G technology

1. Introduction

Here For many years, humans have extracted resources from Earth without discerning environmental concerns. The conversion of combustion automobiles fleet into electric vehicles (EVs) may reduce the arising issues. In addition to that, EVs open new possibilities such as vehicle-to-home (V2H), vehicle-to-vehicle (V2V), and vehicle-to-grid (V2G). Thus, it has started the path for vehicle-to-everything (V2X). Among those approaches, V2G allows

* Corresponding author. Tel.: +55(67) 3743-1000.
E-mail address: ruben.godoy@ufms.br

10.1016/j.trpro.2023.11.014

vehicles to be charged by the grid or supply energy to it, enabling EVs not only to assist in transportation but also to act as controllable loads and distributed energy sources, enabling possibilities for pricing and strategies for peak demand mitigation, which is a hot topic for distribution companies (Liu et al., 2013; Li et al., 2020).

Inside the V2G electric vehicle charging station, there are some power electronics converters. Among them, the bidirectional DC-AC converter allows the correct power flow among EVs and the grid. Its main function is to regulate the internal DC bus to allow the proper operation of the microgrid. From this point of view, this converter must be prepared to inject and/or absorb power from the grid obeying standards while maintaining energy quality aspects. Thus, this converter must be controlled accordingly and for that sense, it is applied a multi-loop current control strategy in the dq axis for active and reactive injection (Pena et al., 2020). Regarding the power converter that feeds energy to the stationary battery bank, it is a bidirectional DC-DC converter (Sreejyothi et al., 2022), with a proper algorithm to charge the batteries, and regarding the power converter that feeds power to the e-bikes, we have used the wireless double LCC topology (Zhang et al., 2019).

This paper presents the microgrid topology and the primary power converters used in the solution. It demonstrates the microgrid's ability to exchange power with the grid through the bidirectional DC-AC converter. The microgrid is supplied by a photovoltaic (PV) source, a stationary battery bank, and wireless charging for e-bikes. Additionally, the paper analyzes all of the microgrid converters and their functions.

2. Methodology

The proposed electric vehicle charging station is a type of DC microgrid with an AC grid interface as illustrated in Figure 1. The energy sources of the microgrid include a PV system, a stationary battery bank, and mobile battery banks resulting from e-bikes. The microgrid also features 10 e-bikes, each with its own wireless power converter (Zhang et al., 2019) for charging. The PV system incorporates a unidirectional DC-DC converter that tracks the maximum power point and increases the voltage to connect it to the DC bus (de Brito et al., 2021). The stationary battery bank is interfaced with the DC bus through a bidirectional current DC-DC converter with buck and boost properties (Sreejyothi et al., 2022).

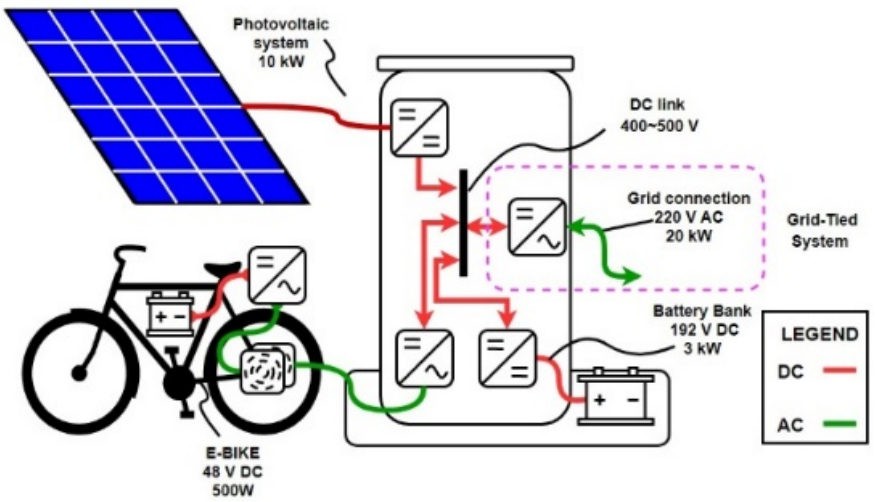

Fig. 1. Proposed microgrid.

The specifications of power and energy of each stage were based on the assumption that the electric charging station is capable of charging until 10 e-bikes with a 15 Ah battery capacity each. If the batteries are charged with a 5 A constant current in a range of 36-48 V and looking for a global efficiency of 80% one may find a power converter of 250 W. In case of grid faults or absence, a stationary battery bank was dimensioned. All e-bikes must be

charged at least once by the stationary bank and, thus, a minimum of 150 Ah capacity is necessary. Assuming a series connection of four 50 Ah / 48 V with a current of 12.5 A for charging one may find a converter of 3 kW. To ensure the sustainability of the electric charging station, a photovoltaic power source was dimensioned to complete four charges of the stationary bank per day. As a result, a 10 kW PV array would be suitable. The PV power can be used to charge the wireless e-bikes, charge the stationary bank, and feed power to the grid through the interleaved converter, allowing the V2G application.

The grid-tied converter consists of two parallel voltage source inverters (VSIs) that can each handle up to 10 kW. This design reduces the current over the grid coupling filters, which can be of the L or LCL types (Volpato et al., 2021). Additionally, this converter works in the interleaved mode to reduce the grid-injected ripple. The topology can be visualized in Figure 2. I_0 represents the currents being injected or absorbed by the remaining converters of the microgrid. Table 1 summarizes the main converter´s specifications.

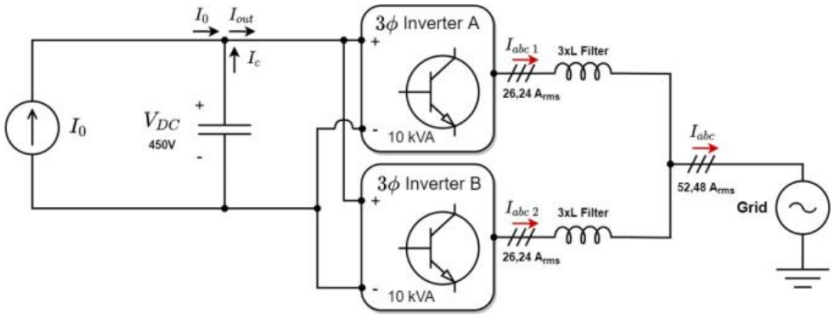

Fig. 2: Interleaved bidirectional DC-AC converter.

Table 1: Interleaved bidirectional DC-AC converter specifications.

Element	Specification
Three-phase VSI	2 x 10 kW
Input Voltage	450 VDC
Capacitance	22 mF/ 700 VDC
Output Filter	520 µH – 27 Arms
Switching frequency	15 kHz
Acquisition frequency	30 kHz

Each converter act as a separate current source connected to the same DC bus. Both inverters have their own current control loop using a synchronous reference frame strategy, where the current controllers can follow the references for injecting or absorbing active or reactive powers. The outer control loop is for voltage regulation. According to the changes in the DC bus voltage (e.g., power injection from the other converters), the controller updates the reference for the current components which is equally divided between the grid-tie converters. The proper regulation of the DC bus allows the remaining converters to properly exchange power with the DC bus. For grid synchronization, it is used a positive sequence phase-locked-loop strategy (Se-Kyo Chung, 2000). The control blocks are depicted in Figure 3. This converter is able to inject active power by means of the Active Power Control block (generating $i_{d\ ref}$) or promote reactive power compensation through the Reactive Power Control block (producing $i_{q\ ref}$). v_{grid} represent the three-phase input voltages, SRF-PLL is the synchronous reference frame phase-locked-loop, θ is the angle for synchronization, Q and Q_{ref} are the reactive power and the reference reactive power, V_{DC} and $V_{DC\ ref}$ are the DC bus voltage and its reference, and SPWM represents the sinusoidal modulation.

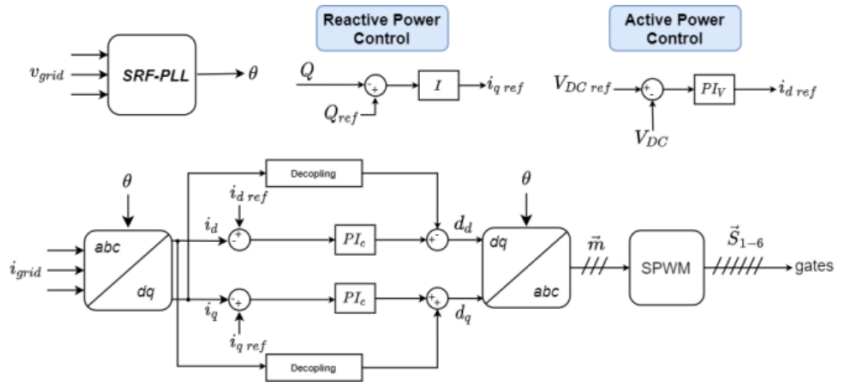

Fig. 3: Control block diagram of the interleaved bidirectional DC-AC converter.

The stationary battery bank-supplied converter is depicted in Figure 4. It is composed of a half-bridge arm with active switches S1 and S2. The convert can reduce the DC voltage to a proper value to charge the batteries or step-up the batteries voltage to feed the DC bus (bidirectional properties). The charging stage is comprised of a two-stage algorithm that deals with a constant-current and a constant-voltage strategy. Thus, the batteries are charged with a constant current until the desired voltage is achieved; in sequence, the constant-voltage stage is initiated to maintain a proper voltage value. One can verify the charge and discharge strategy in Figure 5. Additionally, an input L_F-C_F filter is added to the converter to reduce the ripple current being injected into the DC bus.

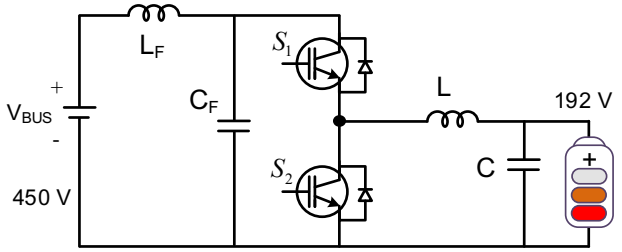

Fig. 4: Bidirectional current DC-DC converter for feeding power to the stationary battery bank.

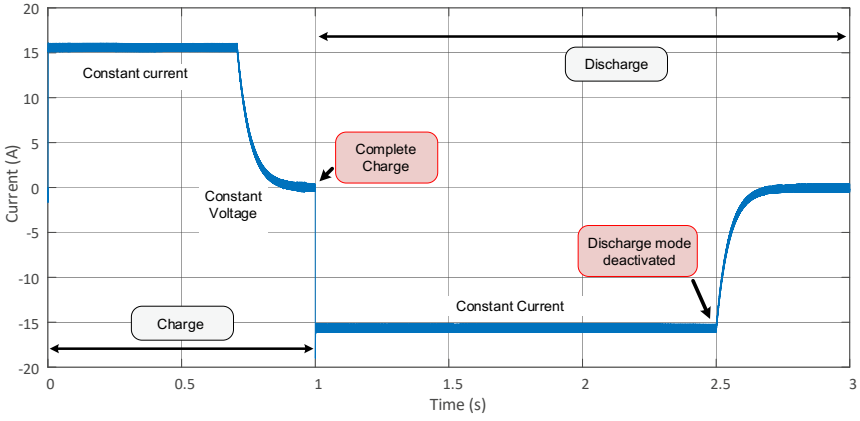

Fig. 5: Charge and discharge strategy.

Table 2 summarizes the main converter's specifications.

Table 2: Bidirectional DC-DC converter specification.

Element	Specification
L_F	320 µH – 7.5 Arms
C_F	3.3 µF – 600 VDC
L	757 µF – 16 Arms
C	180 µF – 250 VDC
Switching frequency	50 kHz
Acquisition frequency	5 kHz

The wireless power converter is shown in Figure 6. One can verify the two VSI converters to allow the bidirectional functionality. To properly compensate for the reactive power of the wireless coils (represented by its magnetizing inductance - M, in this Figure), a double LCC compensation network is adopted. The common compensation strategies as series-parallel and series-series (and their derivations) (Zhang et al., 2022) have their drawbacks and are not symmetrical which reduces their suitability in this application. We would like to emphasize the inherent output current characteristic of the double LCC topology, less instability related to reduced coupling (increase coils distance) and parameter variations, and input and output are symmetrical which allows V2G technology.

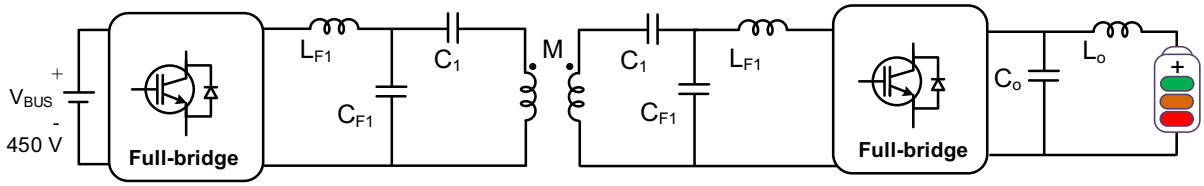

Fig. 6: Bidirectional wireless converter for feeding power to the e-bikes.

Table 3: Bidirectional wireless converter specification.

Element	Specification
L_{F1}	152.3 μH
C_{F1}	26.6 ηF
C1	29.6 ηF
M	360.0 μH
Switching frequency	79 kHz

3. Results and Discussion

The Launchpad F28379D was used to control the grid-tie converter, while a low-cost DsPIC board was used for the remaining converters. Figure 7 shows the results of injecting active power into the grid. In Figure 7(a), one may see the instant of connection to the grid – in yellow, the PLL (phase-locked-loop) signal, in purple, the DC bus voltage – the grid connection instant occurs with 450 V, and in blue and green, it is shown the injected currents. In Figure 7(b), it is displayed the steady-state waveforms – in purple, phase A voltage, and in blue and green, phase A

and B currents. In such experiment, it is shown 1.2 kW power once the DC bus is fed by the stationary battery bank through its bidirectional power converter.

In Figure 8 one can observe the injection of power of almost 8 kW with currents with reduced harmonic content - THD of 4.2%. In this scenario, a TerraSAS PV emulator was added to the system as the PV source for increasing the available power. All grid-injected currents are with reduced harmonic content as observed.

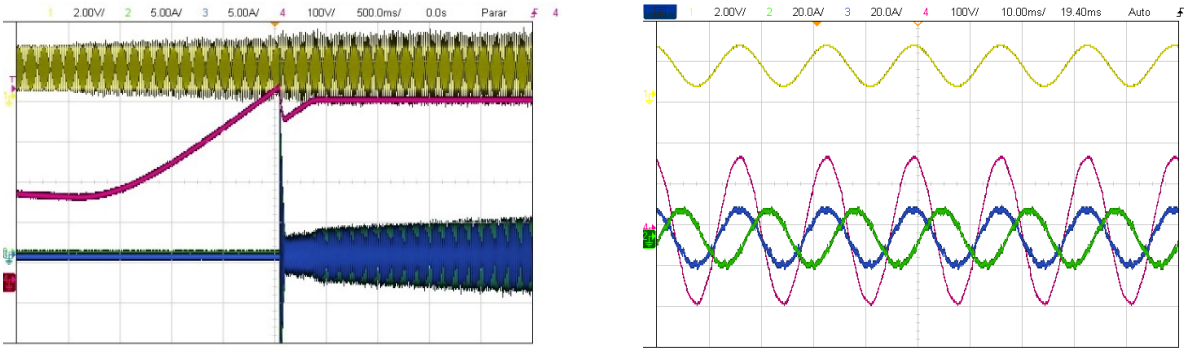

(a) (b)

Fig. 7: Waveforms for grid-connection. (a) Instant of connection. (b) Steady State.

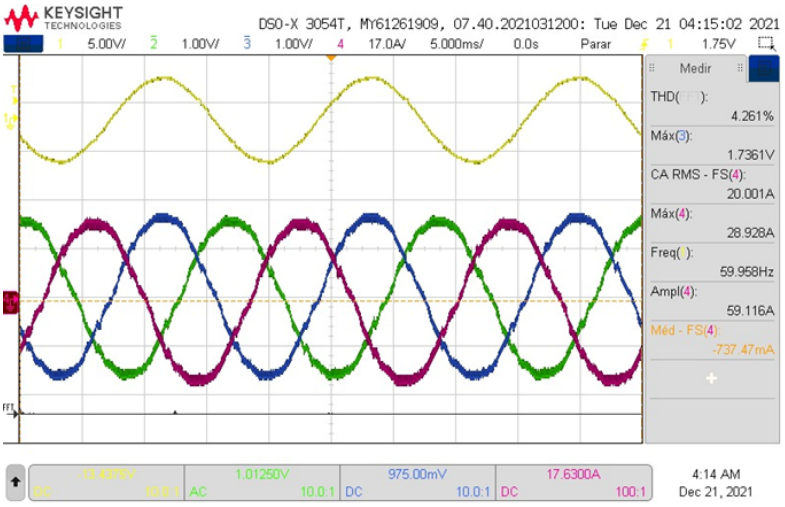

Fig. 8: Waveforms for grid-connection - Steady state. Yellow – PLL output; Green, purple and blue – Grid injected currents.

The waveforms of the stationary battery charger current can be observed in Figures 9(a) and (b). Figure 9(a) shows the charging current during the initiation process until it reaches a desirable constant value, while Figure 9(b) depicts the smooth end of the charging process. In almost 100ms the battery current reduces or increases linearly 3 A.

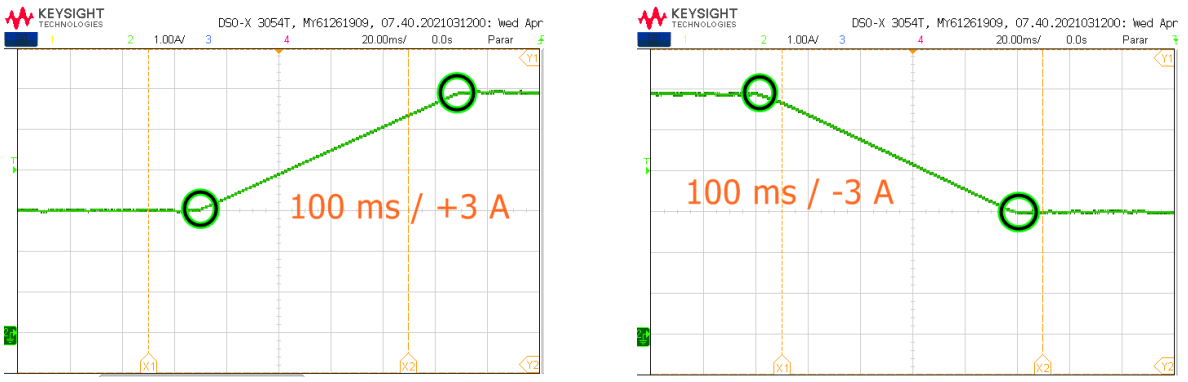

(a) (b)

Fig. 9: Battery charging main waveforms. (a) Charge initiation. (b) Charging ending. 1A/div.

The wireless power converter is tested feeding power to one e-bike with approximately 250 W of output power. In Figure 10(a) one can see the waveforms of voltage and current in the primary coils and in Figure 10(b) one can see the waveforms of voltage and current at the load. The results show the stability of the waveforms as expected by the use of the double LCC compensation.

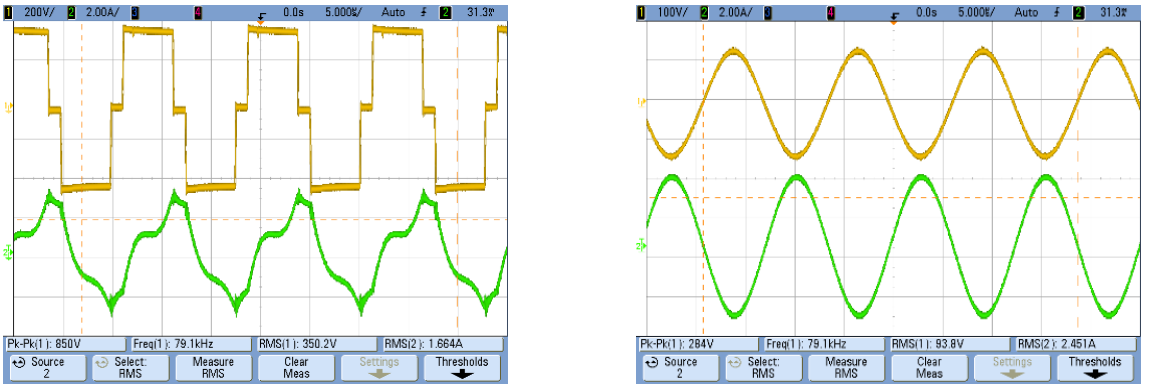

(a) (b)

Fig. 10: Wireless main waveforms. (a) Inverter waveforms. (b) Load waveforms. Voltages in yellow and currents in green. 200V/div and 2A/div.

4. Conclusion

This paper has presented the main power electronics converters of an electric vehicle charging station, which consists of a DC microgrid with an AC interface, as proposed. The EV charger can charge up to 10 e-bikes, store energy in stationary battery banks, and feed renewable power into the grid in V2G mode, up to 20 kW. The bidirectional DC-AC power converter is critical in enabling V2G technology and achieving high-quality active power injection. We have obtained a total harmonic distortion of almost 4% only injecting 8 kW of output power showing the viability of the proposal. Bidirectional charging is suitable for properly charging the stationary bank through the DC-DC converter, while the wireless converter has been tested and can charge e-bike batteries according to the desired current requirement safely, as there is no physical connection.

Acknowledgements

The authors would like to thank Federal University of Mato Grosso do Sul – UFMS and the Research and Development Project-P&D ANEEL. PD-06961-0010/2019.

References

A. S. Volpato, M. A. Souza, F. M. Balta, E. A. Batista, R. B. Godoy, M. A. G. de Brito, Interleaved Bidirectional DC-AC Converter for Electric Vehicle Charging Station. In: 14th IEEE/IAS International Conference on Industry Applications, 2021, São Paulo. INDUSCON. São Paulo: IEEE, 2021. v. 1. p. 1-6.

C. Liu, K. T. Chau, D. Wu and S. Gao, Opportunities and challenges of vehicle-to-home, vehicle-to-vehicle, and vehicle-to-grid technologies, Proceedings of the IEEE, vol. 101, no. 11, pp. 2409--2427, 2013.

J. C. U. Pena, L. P. Sampaio, M. A. G. de Brito and C. A. Canesin, Robust Control of Three-Phase VSI with LCL Filter for Distributed Generation Power Quality Improvement, Journal of Control, Automation and Electrical Systems, vol. 31, pp. 1051--1062, 2020.

K. R. Sreejyothi, Balakrishnakothapalli, K. Chenchireddy, S. A. Sydu, V. Kumar and W. Sultana, Bidirectional Battery Charger Circuit using Buck/Boost Converter, 2022 6th International Conference on Electronics, Communication and Aerospace Technology, Coimbatore, India, 2022, pp. 63-68.

Se-Kyo Chung, A phase tracking system for three phase utility interface inverters, IEEE Transactions on Power Electronics, vol. 15, no. 3, pp. 431--438, 2000.

M. A. G. de Brito, E. A. Batista, V. A. Prado, M. G. Alves, C. A. Canesin, Design Procedure to Convert a Maximum Power Point Tracking Algorithm into a Loop Control System, Energies, v. 14, p. 4550, 2021.

W. Zhang et al., Comparison of Compensation Topologies for Wireless Charging Systems in EV Applications, 2022 International Conference on Artificial Intelligence in Everything (AIE), Lefkosa, Cyprus, 2022, pp. 17-21.

X. Li, Y. Tan, X. Liu, Q. Liao, B. Sun, G. Cao, C. Li, X. Yang and Z. Wang, A cost-benefit analysis of V2G electric vehicles supporting peak shaving in Shanghai, Electric Power Systems Research, vol. 179, p. 106058, 2020.

X. Zhang, J. Wang, M. Xue, Y. Li, and Q. Yang, Research on Dynamic Wireless Charging of Electric Vehicle Based on Double LCC Compensation Mode, 2019 IEEE Wireless Power Transfer Conference (WPTC), London, UK, 2019, pp. 141-145.